Lightweight Deep Learning for Photovoltaic Energy Prediction: Optimizing Decarbonization in Winter Houses

Youssef Jouane, Ilyass Abouelaziz, Imad Saddik, Oussama Oussous

Lightweight Deep Learning for Photovoltaic Energy Prediction: Optimizing Decarbonization in Winter Houses

Youssef JOUANE[a], Ilyass ABOUELAZIZ[b], Imad SADDIK[a], Oussama OUSSOUS[a]

[a] *CESI LINEACT Laboratory UR 7527, Strasbourg, France*
[b] *CESI LINEACT Laboratory UR 7527, Reims, France*

Abstract

This paper proposes an innovative hybrid multivariate deep learning approach to predict photovoltaic (PV) energy production in winter houses, with a focus on lightweight models with low environmental impact. A methodology is developed to assess the carbon footprint of these models, considering training energy consumption, operational CO_2 emissions, and energy savings from PV production optimization. This approach allows selecting models that offer the best trade-off between predictive accuracy and environmental responsibility. The study compares the performance of long short-term memory (LSTM), convolutional neural networks (CNN), and a hybrid CNN-LSTM model for short-term PV production prediction in high-snow regions, using a Positive Energy Winter House (PEWH) case study in Poschiavo, Switzerland. The results show that PV integration can reduce primary energy consumption by up to 63%, with a decarbonization rate of 11%. However, full façade coverage leads to overproduction due to limited winter sunshine and relatively low energy consumption. LSTM optimization identifies configurations (south facade or north roof) achieving decarbonization rates of 131% and 116% respectively, covering 95% to 114% of energy needs, and limiting overproduction. The PEWH case study demonstrates the potential of lightweight deep learning for optimized energy prediction and decarbonization of buildings, especially in cold regions, and highlights the importance of the carbon impact of models in the face of the increasing availability of PV data for more efficient and eco-responsible predictions.

Keywords: Deep Learning, Solar Energy, Decarbonization, Time-Series Forecasting, Building Integrated PV

1. Introduction

The incorporation of passive solar techniques and renewable energy systems into buildings presents a significant potential to decrease energy consumption and tackle environmental issues. Meticulous planning of new constructions and major renovations, considering factors such as insolation, irradiation, and wind direction, can lead to net-zero energy buildings (NZEB). This can result in considerable energy savings, ranging from 20 to 50%, as confirmed by prior studies (1; 2). The optimization of building orientation and geometry is a critical factor in maximizing solar energy production (3). Research carried out by Vassiliades et al. has shown that the prudent orientation of structures enables optimal sunlight capture, thereby contributing to increased renewable energy production (4). Photovoltaic (PV) energy is emerging as a promising renewable energy source for buildings, especially winter houses. However, its production in winter is subject to significant fluctuations due to adverse weather conditions, notably the accumulation of snow on the panels (5). Snow can cause an energy production loss of up to 10% by reflecting more sunlight onto panels (6). This complex phenomenon makes the precise prediction of winter PV production particularly challenging for traditional software. Studies have indicated that PV production losses due to single-face snow amount to an average of 33% in winter and 16% annually (7). These losses underscore the importance of having accurate predictions of PV production for winter house panel integration projects. Previous studies have underscored the effect of sunlight fluctuations and related meteorological variables on the behavior of households equipped with PV panels (8). It is noteworthy that periods of strong sunlight lead to an increase in solar energy consumption. Therefore, accurate prediction of photovoltaic energy production is crucial in winter for optimal energy management in buildings, especially in houses used during the winter. Accurate predictions enable households to better anticipate their energy consumption and adjust their behavior accordingly. Optimizing the integration of PV panels into building-integrated photovoltaic (BIPV) structures involves overcoming technical challenges related to the precise modeling of their performance. Artificial intelligence (AI) emerges as a promising solution to overcome these hurdles and enhance the energy efficiency of BIPV systems (9; 10; 11). Indeed, it provides powerful tools for analyzing complex data and establishing precise predictive models. Studies have demonstrated the potential of AI to accurately predict hourly BIPV power. Polo et al. achieved promising results using XGBoost and Random Forest machine learning models (12). Recent advancements in PV prediction are turning to deep learning approaches, particularly suited to time series (13). Deep learning has advantages over traditional approaches based on predicting solar irradiation and the resulting PV production. While AI shows promise in PV prediction, existing

Email address: yjouane@cesi.fr (Youssef JOUANE)

deep learning models often neglect the complexities of winter conditions, leading to inaccurate predictions in winter houses (14). This limitation is often exacerbated by the use of generic, non-dynamic climate data in prediction software, making accurate predictions challenging, particularly in regions with diverse climates (15). As highlighted by P. Salimi et al., the use of dynamic, localized data is crucial for capturing weather variability and improving prediction accuracy (16). G. Yang et al. further emphasize this point, demonstrating that dynamic, localized weather data can significantly enhance the accuracy of solar energy prediction models, overcoming the limitations of traditional machine learning approaches reliant on generic climate data (17). Recent advances in artificial intelligence (AI), particularly deep learning, offer powerful tools to address these challenges by analyzing complex datasets encompassing weather conditions and panel characteristics, enabling more accurate predictions of PV production. Building on our previous research on deep learning for energy forecasting (see Jouane et al. (13)), the present study uniquely integrates carbon impact assessment into the predictive framework. Although existing research has explored AI for PV prediction, there is a need for models that not only improve prediction accuracy but also prioritize environmental sustainability. Recent advances in PV optimization span both thermal and predictive approaches. For instance, studies integrating nanoscale phase change materials (PCMs) and nanofluidic cooling in PV/T systems (e.g., (18)) demonstrate improved efficiency through hybrid thermal models and neural network forecasts. Parallel work, such as (19), leverages AI for PV prediction in complex environments but overlooks the environmental cost of AI itself. While our study does not address PV/T thermal dynamics, we advance PV efficiency by proposing a hybrid CNN-LSTM model for short-term predicting and introducing a carbon footprint assessment framework. This dual focus balancing prediction accuracy with model sustainability addresses a critical gap in AI-driven PV research. By aligning predictive performance with low carbon AI practices, our work complements thermal efficiency innovations, offering a holistic approach to sustainable PV system design.

Related Works

Existing research addresses the environmental impact of photovoltaic (PV) systems and the carbon footprint of AI models, providing valuable context for this study. Studies on the life-cycle assessment (LCA) of PV systems have explored emissions from manufacturing to disposal, quantifying greenhouse gas (GHG) emissions and comparing them to fossil fuels (as shown in the table 1) (20; 21). These analyses highlight the potential for emission reductions through material innovations and recycling (20). Furthermore, research on PV's decarbonization potential emphasizes its role in optimizing energy structure and reducing reliance on fossil fuels (22; 21). Huo et al. (21) specifically examines the contribution of PV to China's carbon peak target, emphasizing the importance of accurate PV generation predicting for policy decisions. In parallel, the burgeoning field of "Carbon Impact Assessment of AI Models" examines the energy consumption and CO_2 emissions of AI model training and deployment. Studies have investigated the carbon footprint of various machine learning models, including large language models (23; 24; 25), highlighting the energy demands and environmental implications of complex AI. These works often utilize tools like CodeCarbon (25; 23)for emissions tracking, advocating for sustainable AI practices. Martiny et al. (25) notably explores energy consumption patterns of different ML algorithms, including LSTM for time-series data, using CodeCarbon to monitor emissions.

This study distinguishes itself by integrating the carbon impact assessment of AI models with optimized PV production prediction, particularly in challenging winter conditions. Unlike prior work focusing solely on PV's lifecycle emissions or the general carbon footprint of AI, we combine both aspects for a more sustainable and accurate PV integration. By using a hybrid deep learning approach, evaluating the carbon footprint of different models, and employing TOPSIS for model selection based on both performance and environmental impact, this study contributes a more holistic and environmentally responsible framework for PV energy prediction.

This paper presents a innovative hybrid multivariate deep learning approach to predict PV energy production in winter homes under winter conditions, with a focus on energy-efficient models with minimal environmental impact. Careful selection of models and optimizers for accurate solar energy prediction is essential to this approach, contributing significantly to the optimization and planning of solar energy systems under harsh winter conditions. We present a methodology to assess the environmental footprint of these models, considering factors such as material consumption and CO_2 emissions, with the aim of minimizing their negative environmental impact while maximizing predictive performance. This focus on the selection of environmentally friendly models underlines the relevance of the study for the field of renewable energy.

Key Contributions of the Study

This study proposes several notable advances in the field of low greenhouse gas emission photovoltaic (PV) production predicting and in favor of maximum decarbonization:

- **Hybrid methodology and carbon impact assessment**: We propose a new methodology combining a hybrid CNN-LSTM model and a Carbon Impact Assessment of Models for a more accurate and eco-responsible prediction. This approach takes into account both predictive performance and environmental sustainability.

- **TOPSIS-based model selection**: We use the TOPSIS method to select the best performing and least environmentally impactful model among different deep learning models. This multi-criteria approach allows for a more informed and objective selection. This is particularly relevant given that future work is oriented towards exploiting the increasing availability of production and irradiation data, requiring the selection of low-impact models.

Table 1: Comparison of Related Work with This Study

Study	Focus	Methodology	Key Findings/Contributions
(22)	Impact of PV innovation on CO_2	Econometric analysis	PV innovation correlated with CO_2 reduction
(20)	LCA of PV systems	LCA calcul method of decarbonization	PV's lower carbon footprint vs. fossil fuels
(23)	Carbon footprint of AI models	CodeCarbon	AI Models have significant carbon footprint
(24)	Carbon emissions of ML models	Empirical analysis	ML training has environmental costs
(21)	PV's contribution to carbon peak	BiLSTM forecasting, scenario analysis	PV crucial for achieving carbon peak targets
(25)	Sustainable AI, energy consumption of ML	Empirical analysis, CodeCarbon	Strategies for reducing ML energy consumption
This Study	Optimized and decarbonized PV energy integration in the PEWH	Hybrid deep learning, Carbon Impact Assessment, TOPSIS, Decarbonization Method	Accurate and low-carbon LSTM model for PV prediction, with optimized panel placement enhancing energy decarbonization for the PEWH (Positive Energy Winter House).

- **PV Panel Placement Optimization**: We demonstrate the importance of PV panel placement optimization to maximize energy production and decarbonization, particularly in cold regions. The PEWH case study highlights the significant gains achievable through strategic placement.
- **Winter Conditions Analysis**: This study specifically addresses the challenges of predicting PV production in winter conditions, taking into account factors such as limited sunlight and snow accumulation.

The primary objective of this study is to develop an AI-driven methodology that enhances the accuracy of PV energy predicting in winter houses while minimizing the carbon footprint of model training. By integrating a hybrid CNN-LSTM deep learning model, a carbon impact assessment, and the TOPSIS decision framework, The aim is to provide a sustainable and high-precision solution for optimizing PV integration in cold-climate buildings." It is noteworthy the primary objective of this research is to address a critical challenge in solar energy systems: the accurate prediction of PV energy production in winter houses, particularly in high-snow regions. The deep learning models are tools used to achieve this goal, but the core focus remains on optimizing PV energy production, improving energy efficiency, and enhancing decarbonization in building key topics within the solar energy domain. The paper is structured as follows: Section 2 details the scientific methodology, encompassing the architectures of the deep learning models (CNN, LSTM, and the proposed hybrid CNN-LSTM) and the carbon impact assessment methodology, which considers hardware energy consumption (CPU, GPU, RAM), CO_2 emissions from electricity production, and potential energy savings from PV production optimization. Section 3 describes the experimental setup, including the training data process, performance metrics, and the dataset used. Section 4 presents the results and discussion, covering the environmental impact assessment, model ranking using TOPSIS, performance comparison with conventional software (PVsyst, BIMSolar), and analysis of energy efficiency and decarbonization potential under various PV panel placement scenarios. This integrated approach, balancing predictive accuracy with environmental responsibility, aims to contribute to a more sustainable solar energy prediction framework. Our findings highlight the importance of considering the full environmental footprint of predictive models, especially given the increasing availability of PV production and irradiation data, paving the way for more informed and environmentally conscious model selection in future research.

2. Scientific Methodology

2.1. Methodological architecture

In this research, data collected from the Positive Energy Winter House (PEWH) to analyze PV energy production. The power output of the system was meticulously documented at five-minute intervals, measured in kilowatt-hours (KWh), and stored in a dedicated database. Located in Poschiavo, Switzerland, within the canton of Grisons, as depicted in Fig. 1, the winter house is equipped with PV panels seamlessly integrated across its facades and roof. This comprehensive setup encompasses a total of 435 panels, resulting in an impressive annual production capacity of approximately 45,000 kWh.

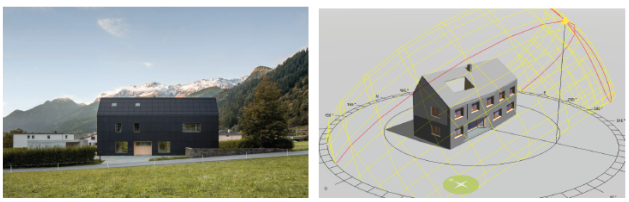

Figure 1: PEWH equipped with PV panels.

The overarching framework of our methodology is illustrated in Fig. 2. The novelty of this study lies in the advancement of

a multivariate approach for short-term PV prediction using artificial deep learning models, tailored to optimize performance. This approach enables us to predict solar power in the extremely short term, requiring a brief training period on multivariate time series. Essentially, the study seeks the most effective approach for a winter house to predict production, emphasizing both prediction accuracy and efficient training. The evaluation of our models incorporates metrics such as Mean Absolute Error (MAE), Root Mean Square Error (RMSE), and Mean Square Error (MSE). In our context, an optimal model is characterized by minimal MAE and a reduced training duration. In Fig. 2, we introduce a innovative method for predicting PV production in the Positive Energy Winter House (PEWH), utilizing a multivariate approach. Precision in prediction is crucial over very short periods and extended training intervals, considering multivariable input data that incorporates meteorological data, location, orientation, and Building Information Modeling (BIM) data of the house. Furthermore, our hybrid approach is distinguished by the combination of a convolutional neural network (CNN) and a long short memory neural network (LSTM). The CNN allows to extract spatial features from meteorological and irradiance data, while the LSTM models the temporal dependencies of PV production time series. This synergy, inspired by recent studies (see for example (14), (17)), aims to significantly improve the accuracy of forecasts in winter conditions while reducing the environmental cost of artificial intelligence models.

2.2. Deep Learning models

In this work, we compare three deep learning approaches for short-term prediction of PV production: (i) the LSTM model, adapted to capture temporal dynamics; (ii) the CNN model, which extracts spatial features from the input data; and (iii) a hybrid CNN-LSTM architecture that combines these two approaches and shows the interest of hybridization to improve the accuracy and robustness of forecasts in complex environments (14).

2.2.1. Convolutional Neural Network (CNN):

The convolutional neural network (CNN) is a fundamental component of artificial neural networks, renowned for its adeptness in various applications, notably excelling in tasks like facial and vocal emotion recognition, where it demonstrates an impressive capacity for extracting intricate features (26; 27). However, its utility extends far beyond these domains; it proves to be remarkably effective in the domain of short-term PV energy prediction as well. This assertion finds support in the work of Yuchi, S. et al., who devised a proficient CNN-based model specifically tailored for predicting PV energy at 15-minute intervals (28).

The architecture of the CNN model is structured around four fundamental layers, each serving a unique function: the convolution layer, pooling layer, rectified linear unit (ReLU) activation layer, and fully-connected layer. The convolution layer acts as the backbone of the CNN, responsible for detecting patterns and features within the input data through convolution operations. These operations involve applying a set of learnable filters to the input data, resulting in feature maps that highlight relevant spatial patterns. Following the convolution layer, the pooling layer plays a pivotal role in downsampling the feature maps, reducing their spatial dimensions while preserving essential information. Common pooling techniques include max pooling and average pooling, which help to enhance the network's translational invariance and reduce computational complexity.

The rectified linear unit (ReLU) activation layer introduces non-linearity into the network by applying the ReLU function element-wise to the feature maps. This activation function enhances the model's capability to capture complex relationships within the data, promoting faster convergence during training and mitigating the vanishing gradient problem. The ReLU function sets all negative values to zero while leaving positive values unchanged, resulting in sparse, more discriminative representations.

Finally, the fully-connected layer, also known as the dense layer, serves as the interface between the convolutional layers and the output layer, facilitating the transformation of the high-level features extracted by the preceding layers into predictions or classifications. Each neuron in the fully-connected layer is connected to every neuron in the preceding layer, allowing for comprehensive information integration and abstraction. By leveraging the combined functionality of these key layers, the CNN architecture proves to be a formidable tool for short-term PV energy prediction, enabling the extraction of relevant temporal and spatial features from solar irradiance and other relevant meteorological data, thereby enhancing the accuracy and robustness of the prediction model.

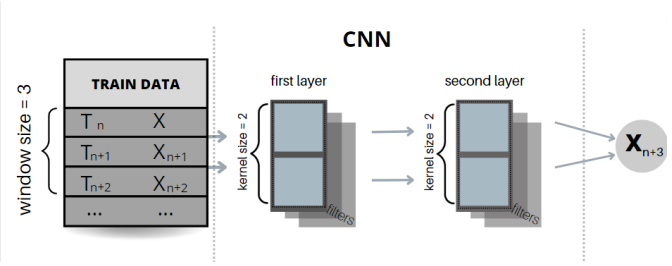

Figure 3: CNN architecture.

2.2.2. Long Short-Term Memory (LSTM):

Long Short-Term Memory (LSTM) is a type of Recurrent Neural Network (RNN) designed to effectively learn and remember long-term dependencies in sequential data (29). It is widely recognized as a prominent example in predictive modeling, as noted by Hochreiter and Schmidhuber (30). LSTM's efficacy lies in its ability to address various challenges in time series prediction, accommodating both univariate and multivariate scenarios. Its distinctive architecture, which includes a central cell state and three essential gates, enables LSTM to selectively assimilate, release, or retain information. This unique feature enhances its capacity to recognize and model complex temporal patterns, making LSTM especially effective at understanding and modeling complex temporal patterns within data. The architecture of this model is illustrated in Fig. 4, with the

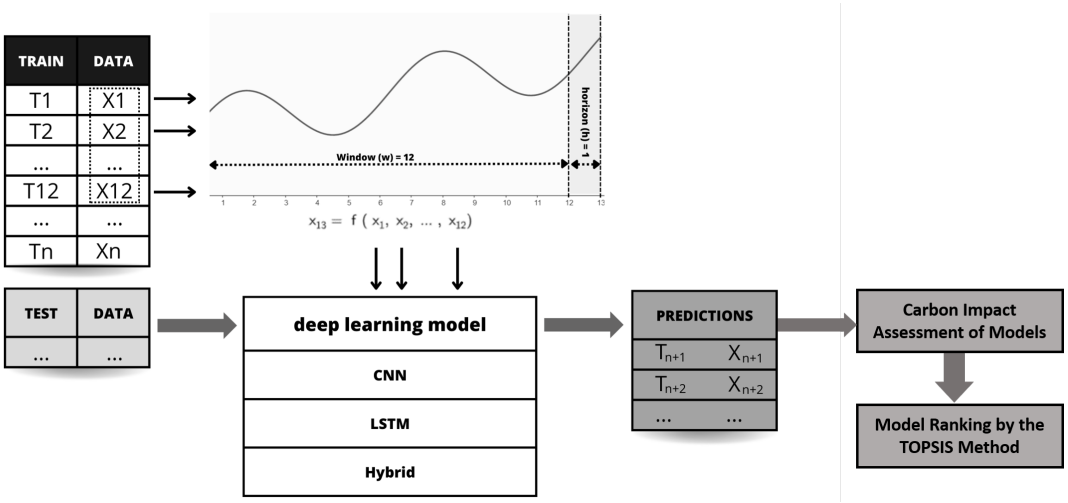

Figure 2: Architecture of the proposed methodology.

following parameters: C_{t-1}: memory at time $t-1$; C_t: memory at time t; h_t: hidden layer at time t; h_{t-1}: input to hidden layer $t-1$; X_t: cell input; σ and tanh are activation functions used in neural networks.

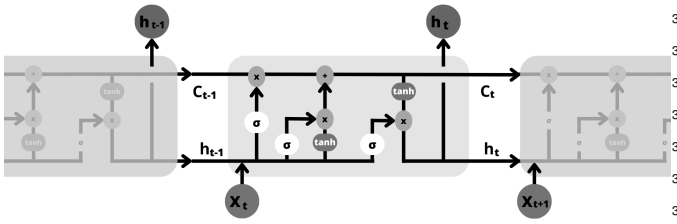

Figure 4: LSTM architecture.

2.2.3. *Hybrid model (CNN-LSTM):*

The integration of hybrid models combining the convolutional neural Network and the LSTM network presents a significant advantage by combining the strengths of both paradigms. A hybrid approach is explored in which CNN and LSTM are synergistically used for enhanced time series prediction.The architecture of the proposed hybrid model that we call **ConvL-STM** is illustrated in Fig. 5. The model integrates two distinct phases: feature extraction and sequential learning.

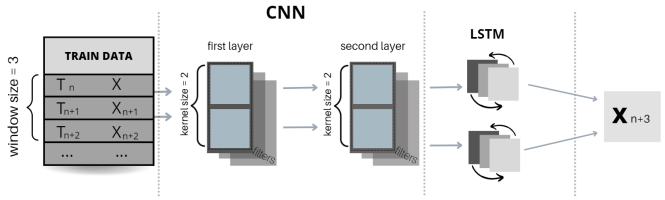

Figure 5: Architecture of the hybrid model.

First, the CNN component is employed to extract significant features from the input time-series data. CNNs are adept at identifying and capturing spatial hierarchies and patterns, which makes them highly effective in preprocessing time-series data to highlight important features. Following feature extraction, the identified features are fed into the Long Short-Term Memory (LSTM) network. LSTMs are designed to handle and learn from sequential data by capturing temporal dependencies and long-range relationships. This phase enables the model to analyze and predict based on the sequential nature of the features extracted by the CNN. This hybrid approach proves to be effective for handling complex time series datasets. The CNN's role in extracting relevant features enhances the LSTM's ability to manage and learn from sequential data. This combination allows the model to achieve a high level of accuracy and robustness in prediction tasks. A critical aspect of our study is the refinement of the model's hyperparameters. Key parameters such as the number of convolutional filters, kernel sizes, the number of LSTM units, learning rates, and regularization techniques have been meticulously optimized. This optimization process aims to improve the model's performance and ensure its effectiveness across diverse and complex time series datasets.

2.3. *Carbon Impact Assessment of Models*

In order to quantify the environmental impact of our deep learning models, the Python library CodeCarbon was integrated. This allows us to measure the energy consumption of the hardware (CPU, GPU, RAM) during training, by taking periodic readings. The associated CO_2 emissions are calculated via a carbon intensity factor (gCO_2eq/kWh), based on the regional energy mix obtained from public data sources. The training time is also analyzed, since a reduction in computation time directly reduces the carbon footprint. This approach, aligned with recent work (25), provides a transparent and reproducible assessment, essential for models deployed at large scale.
Fig. 6 illustrates CodeCarbon's methodology: energy consumption (in kWh) is multiplied by the carbon intensity of electricity (in gCO_2eq/kWh) to estimate total CO_2 emissions. In the absence of specific regional data, CodeCarbon uses a global

average value. CodeCarbon's minimal impact on performance is a key advantage. Its scheduler periodically measures energy consumption, ensuring negligible overhead on the main application. This allows for seamless integration of emissions monitoring into Python code, without significantly impacting performance or requiring major changes. While CodeCarbon is a valuable tool, it has limitations. Like any tool, it relies on assumptions and approximations. For example, for processors not referenced in its database, CodeCarbon uses a constant value. Similarly, in the absence of precise data on the carbon intensity of the local electricity grid, it uses global average values. Despite these limitations, CodeCarbon remains a powerful and accessible solution for quantifying the environmental impact of model development. Other methodologies, such as life cycle assessment (LCA) and product carbon footprint calculations, offer alternative approaches. As the technology industry increasingly places emphasis on sustainability, we can expect more sophisticated tools and best practices to emerge, improving the accuracy of emissions tracking and providing a more comprehensive understanding of the carbon footprint of software projects. Our method for calculating CO_2eq emissions, illustrated in Fig. 6, follows an approach commonly used in the life cycle assessment (LCA) of information and communication technologies (ICT) (31). It consists of multiplying energy consumption (kWh) by the carbon intensity of the electricity mix (gCO_2eq/kWh) (32), which reflects the average greenhouse gas emissions per unit of electricity produced, taking into account the energy mix (33).

3. Experimental Setup

3.1. Training

Four models (ANN, CNN, ConvLSTM, and LSTM) were trained to predict the PV energy production of the winter house. The architectures of these models are detailed in Fig. 7. The ANN model is composed of three densely connected layers, each designed to progressively extract and learn features from the input data, followed by an output layer that generates the final predictions. The CNN model consists of two convolutional layers that specialize in capturing spatial features from the input data. These layers are followed by a dense layer, which further processes the extracted features, and an output layer that provides the final output. The LSTM model is structured with two LSTM unit layers, which are particularly effective for capturing temporal dependencies in sequential data. These layers are followed by an output layer that produces the final prediction. Finally, the hybrid model combines elements of both convolutional and recurrent networks by incorporating two ConvLSTM1D layers. These layers blend convolutional operations with LSTM units to capture both spatial and temporal patterns in the data. The ConvLSTM1D layers are followed by a dense layer and an output layer, which together deliver the final prediction. Table. 3 details the parameter count for each model, providing an indication of their respective complexities. The ANN model consists of 95,555 parameters, highlighting its relatively lower complexity in comparison to the other models.

Table 2: Dataset description.

Parameters	**Description**	**Units**
Air temp	The air temperature at 2 meters above surface level	$^{\circ}C$
Albedo	The average daytime surface reflectivity of visible light	$0-1$
Azimuth	The angle between the horizontal direction of the sun, and due north	$^{\circ}$
Clearsky DHI	The diffuse irradiance received on a horizontal surface (if there are no clouds)	W/m^2
Clearsky DNI	The direct irradiance received on a horizontal surface (if there are no clouds)	W/m^2
Clearsky GHI	Total irradiance on a horizontal surface (if there are no clouds). The sum of direct and diffuse irradiance components received on a horizontal surface	W/m^2
Clearsky GTI	Total irradiance received on a surface (if there are no clouds), with defined tilt and azimuth (sum of direct, diffuse and reflected components), fixed or tracking.	W/m^2
Cloud opacity	The attenuation of incoming sunlight due to cloud	$\%$
Dewpoint temp.	The dewpoint temperature at 2 meters above surface level	$^{\circ}C$
DHI	The diffuse irradiance received on a horizontal surface	W/m^2
DNI	Irradiance received from the direction of the sun	W/m^2
GHI	Total irradiance on a horizontal surface. The sum of direct and diffuse irradiance components received on a horizontal surface	W/m^2
GTI	Total irradiance received on a surface with defined tilt and azimuth (sum of direct, diffuse and reflected components), fixed or tracking.	W/m^2
Precipitation water	Precipitable water of the entire atmospheric column.	Kg/m^2
Precipitation rate	An estimate of the average precipitation rate	mm/h

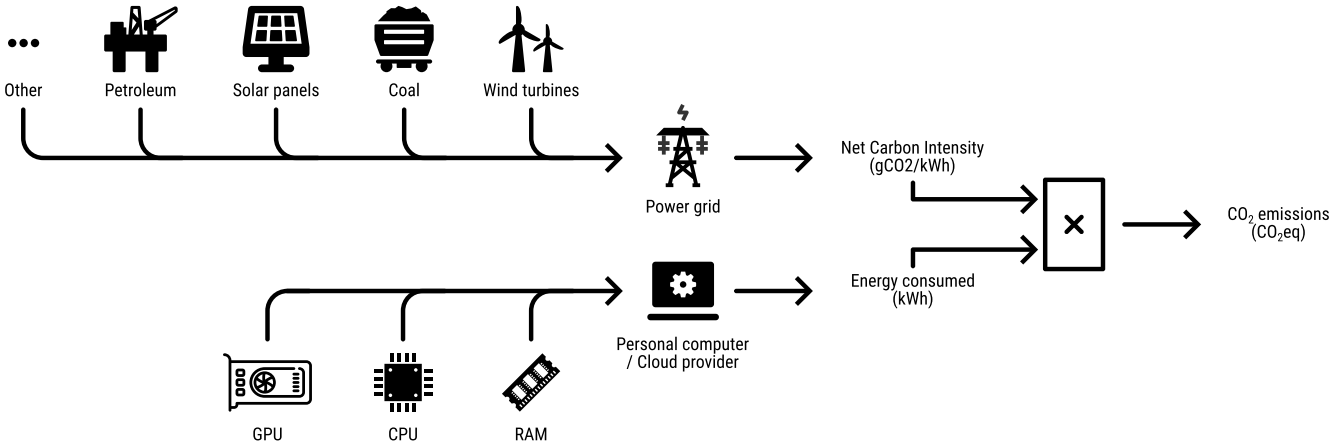

Figure 6: CodeCarbon methodology.

The CNN model, with 206,849 parameters, demonstrates a significantly more complex architecture. The Long LSTM model occupies an intermediate position, with a total of 129,345 parameters. In contrast, the ConvLSTM model, with 60,801 parameters, exhibits the lowest parameter count among the models analyzed. These differences in parameter counts underscore the varying levels of architectural complexity across the models. Having fewer parameters in the ConvLSTM model offers several advantages, including reduced computational complexity and improved generalization. A model with fewer parameters generally requires less memory and computational power, leading to faster training and inference times. This efficiency is particularly beneficial in resource-constrained environments and for real-time applications. Additionally, fewer parameters reduce the risk of overfitting, as the model is less likely to memorize noise from the training data, thereby improving its performance on unseen data. This reduction in parameter count also simplifies the hyperparameter tuning process and can lead to more stable training, enhancing the model's robustness and interpretability.

Model	Parameter Count
ANN	95,553
CNN	206,849
LSTM	129,345
ConvLSTM	60,801

Table 3: Parameter counts for each model, reflecting their respective complexities.

To ensure a fair comparison among the models, the training procedures were standardized across all models. For training, the Adam optimizer was used with a learning rate set to $10e^{-}3$. Each model was trained for 50 epochs with a batch size of 512, and the training was conducted on a single Tesla T4 GPU. This setup ensures consistent and comparable performance metrics for each model, facilitating a thorough evaluation of their prediction capabilities. Our model assessment strategy involves dividing the data into 80% for training, 10% for validation, and 10% for testing. This approach ensures a robust evaluation by allowing the model to learn from the majority of the data, while the validation set is used to fine-tune the model's hyperparameters and prevent overfitting. Finally, the testing set provides an unbiased assessment of the model's performance on unseen data, giving us a clear indication of how well it is likely to generalize to new, real-world data.

3.2. Metrics

To evaluate the performance of the models in prediction PV energy production, several key metrics are used. Each metric is defined as follows:

- **R-squared** (R^2): This metric measures the proportion of variance in the target variable that is explained by the model. It is calculated as:

$$R^2 = 1 - \frac{\sum_{i=1}^{n}(y_i - \hat{y}_i)^2}{\sum_{i=1}^{n}(y_i - \bar{y})^2} \tag{1}$$

  where:

  - y_i is the actual value for the i-th observation,
  - $\hat{y}_i$ is the predicted value for the i-th observation,
  - $\bar{y}$ is the mean of the actual values,
  - n is the number of observations.

  The R^2 metric, used to evaluate model performance, is defined in Equation 1. An R^2 value of 1 indicates that the model explains all the variance, while a value of 0 indicates no explanatory power.

- **Mean Absolute Error (MAE)**: This metric measures the average magnitude of errors in predictions, without considering their direction. The MAE is computed using Equation 2. It is given by:

$$MAE = \frac{1}{n}\sum_{i=1}^{n}|y_i - \hat{y}_i| \tag{2}$$

  where:

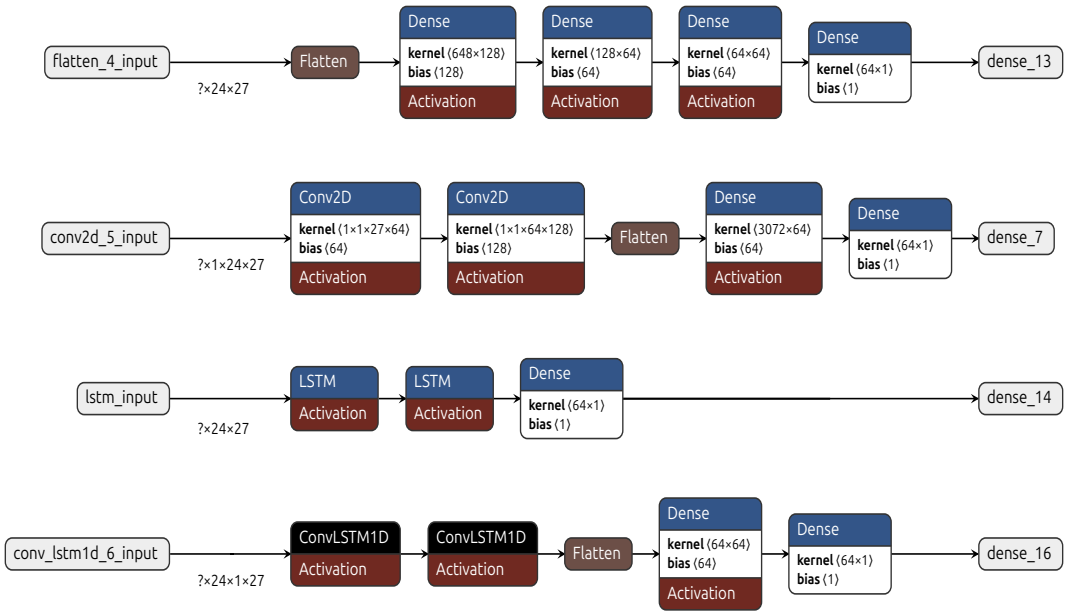

Figure 7: A detailed look at the architecture of each one of the used models.

  - n is the number of observations,
  - $|y_i - \hat{y}_i|$ is the absolute error for the i-th observation.

- **Mean Squared Error (MSE)**: This metric measures the average squared difference between predicted and actual values, giving more weight to larger errors. The MSE is given by Equation 3 and calculated as:

$$MSE = \frac{1}{n}\sum_{i=1}^{n}(y_i - \hat{y}_i)^2 \tag{3}$$

where:

  - n is the number of observations,
  - $(y_i - \hat{y}_i)^2$ is the squared error for the i-th observation.

- **Root Mean Squared Error (RMSE)**: This metric is the square root of the MSE and provides a measure of the average magnitude of the errors, expressed in the same units as the target variable. The RMSE is determined using Equation 4. It is computed as:

$$RMSE = \sqrt{\frac{1}{n}\sum_{i=1}^{n}(y_i - \hat{y}_i)^2} \tag{4}$$

where:

  - n is the number of observations,
  - $(y_i - \hat{y}_i)^2$ is the squared error for the i-th observation.

- **Mean Absolute Percentage Error (MAPE)**: This metric calculates the average absolute percentage error relative to the actual values, providing insight into the model's accuracy across different scales. The MAPE is given in Equation 5. It is given by:

$$MAPE = \frac{100\%}{n}\sum_{i=1}^{n}\left|\frac{y_i - \hat{y}_i}{y_i}\right| \tag{5}$$

where:

  - n is the number of observations,
  - $\left|\frac{y_i - \hat{y}_i}{y_i}\right|$ is the absolute percentage error for the i-th observation.

These collective metrics provide a comprehensive guide to choosing the best performing model, based on the accuracy of its predictions and the characteristics of its errors. The parameters of the measures used in the equations are summarized in Table 4.

Symbol	Description
y_i	Actual value of the i-th observation
$\hat{y}_i$	Predicted value of the i-th observation
$\bar{y}$	Mean of actual values
n	Total number of observations
R^2	Coefficient of determination
MAE	Mean Absolute Error
MSE	Mean Squared Error
$RMSE$	Root Mean Squared Error
$MAPE$	Mean Absolute Percentage Error

Table 4: Summary of notation used in the equations.

3.3. Dataset

The dataset used for training the models includes meteorological data and PV energy production (table 2), with the latter

being the target variable.

Meteorological Data: This includes various weather-related features that are essential for prediction PV energy production. The data points include, but are not limited to, temperature, humidity, wind speed, and solar radiation. These variables are crucial for understanding the environmental conditions impacting PV energy generation.

PV Energy Production: This is the target variable of our prediction models. It represents the amount of energy produced by the PV system and is recorded at regular intervals. Accurate prediction of this variable is critical for optimizing energy management and planning. The meteorological data was obtained from the Solcast platform and spans from July 1st, 2021, to May 31st, 2022. This dataset comprises a total of 28 columns, which are detailed in Table. 2.

4. Results and discussions

4.1. Environmental Impact Assessment: Energy Consumption and CO_2 Emissions

This section presents a comprehensive evaluation of the performance and environmental impact of the LSTM, ANN, CNN, and ConvLSTM models. Fig. 8 illustrates the performance of each model, using the metrics defined in Section 3.2. The hybrid model is distinguished by an R^2 score comparable to that of the LSTM model, but with a smaller number of parameters, suggesting better resource efficiency. The model performance evaluation, presented in Fig. 8, indicates that the hybrid model offers promising results. Indeed, the hybrid CNN-LSTM model achieves the best predictive accuracy with an R^2 of 0.975, outperforming the standalone CNN (R^2 = 0.928) and the LSTM (R^2 = 0.971), confirming that the integration of spatial and temporal feature extraction improves robustness, especially in fluctuating winter conditions. The RMSE and MAE values indicate that the CNN-LSTM model maintains lower prediction errors compared to other models, which is particularly relevant for managing energy storage and grid stability in winter houses. The MAPE metric highlights that prediction accuracy decreases slightly during extreme snow conditions, requiring adaptive training strategies. However, a more detailed analysis of its environmental impact, performed using the CodeCarbon library (Section 2.3) and illustrated in Fig. 9, reveals unexpected complexity. Indeed, while the hybrid model initially seems lighter in terms of parameters, its carbon footprint is not systematically the lowest. This observation highlights the need for a multidimensional assessment of deep learning models, taking into account both technical and environmental aspects. To assess the environmental impact, we analyzed the energy consumption and corresponding CO_2 emissions during model training, using the CodeCarbon library (described in Section 2.3) (Fig. 9). CodeCarbon measures the energy consumption of the hardware (CPU, GPU, RAM) and calculates CO_2 emissions based on the carbon intensity of the local electricity grid. Although the hybrid model initially seems greener, a deeper analysis of its training time and energy consumption reveals that it is not necessarily the optimal choice.

4.2. Model Ranking by the TOPSIS Method

In order to obtain a comprehensive ranking of models, taking into account both performance and environmental impact, we applied the TOPSIS method (34). TOPSIS, a multi-criteria analysis method using compensatory aggregation, compares alternatives by weighting the criteria, normalizing the scores, and calculating the geometric distance to an ideal solution. This approach allows ranking models according to their proximity to this ideal solution, by considering several often contradictory criteria (35). The steps of the TOPSIS method are detailed below:

1. **Decision Matrix:** This matrix X is constructed with m models (rows) for n criteria (columns), with x_{ij} as the performance of model i with respect to criterion j.
2. **Weights:** A weight w_j is assigned to each criterion to indicate its importance. The weights are usually chosen to sum to 1 and are shown in table 5.
3. **Normalization:** The decision matrix is normalized to form the matrix $R = [r_{ij}]$, with $r_{ij} = \frac{x_{ij}}{\sqrt{\sum_{i=1}^{m} x_{ij}^2}}$.
4. **Weighted Normalized Decision Matrix:** Each normalized criterion is then multiplied by its respective weight to obtain the weighted normalized decision matrix $V = [v_{ij}]$, with $v_{ij} = w_j \cdot r_{ij}$.
5. **Ideal and Negative-Ideal Solutions:** The ideal solution A^* and negative ideal solution A^- are defined as $A^* = \{v_{1j}^*, v_{2j}^*, ..., v_{nj}^*\}$ and $A^- = \{v_{1j}^-, v_{2j}^-, ..., v_{nj}^-\}$, where for all j except for the R2 score, $v_j^* = \min_i(v_{ij})$ and $v_j^- = \max_i(v_{ij})$, and for the R2 score, $v_j^* = \max_i(v_{ij})$ and $v_j^- = \min_i(v_{ij})$.
6. **Separation Measures:** The separation from the ideal solution S_i^+ and the separation from the negative ideal solution S_i^- are calculated as $S_i^+ = \sqrt{\sum_{j=1}^{n}(v_{ij} - v_j^*)^2}$ and $S_i^- = \sqrt{\sum_{j=1}^{n}(v_{ij} - v_j^-)^2}$.
7. **Relative Closeness to the Ideal Solution:** The relative closeness of the alternative i with respect to A^* is calculated as $C_i = \frac{S_i^-}{S_i^+ + S_i^-}$.
8. **Rank the Preference Order:** The alternatives are ranked according to C_i, and the one with the highest C_i is chosen.

Applying the TOPSIS method to the four models (LSTM, ANN, CNN, and ConvLSTM) based on their performance metrics yielded the following proximity coefficients:

- LSTM: 0.836265
- ANN: 0.801073
- CNN: 0.692485
- ConvLSTM: 0.314679

A higher coefficient indicates a better model. The LSTM model is therefore the best performer according to our TOPSIS analysis.

The TOPSIS proximity coefficients (LSTM: 0.83; Hybrid CNN-LSTM: 0.31) highlight a crucial challenge in sustainable

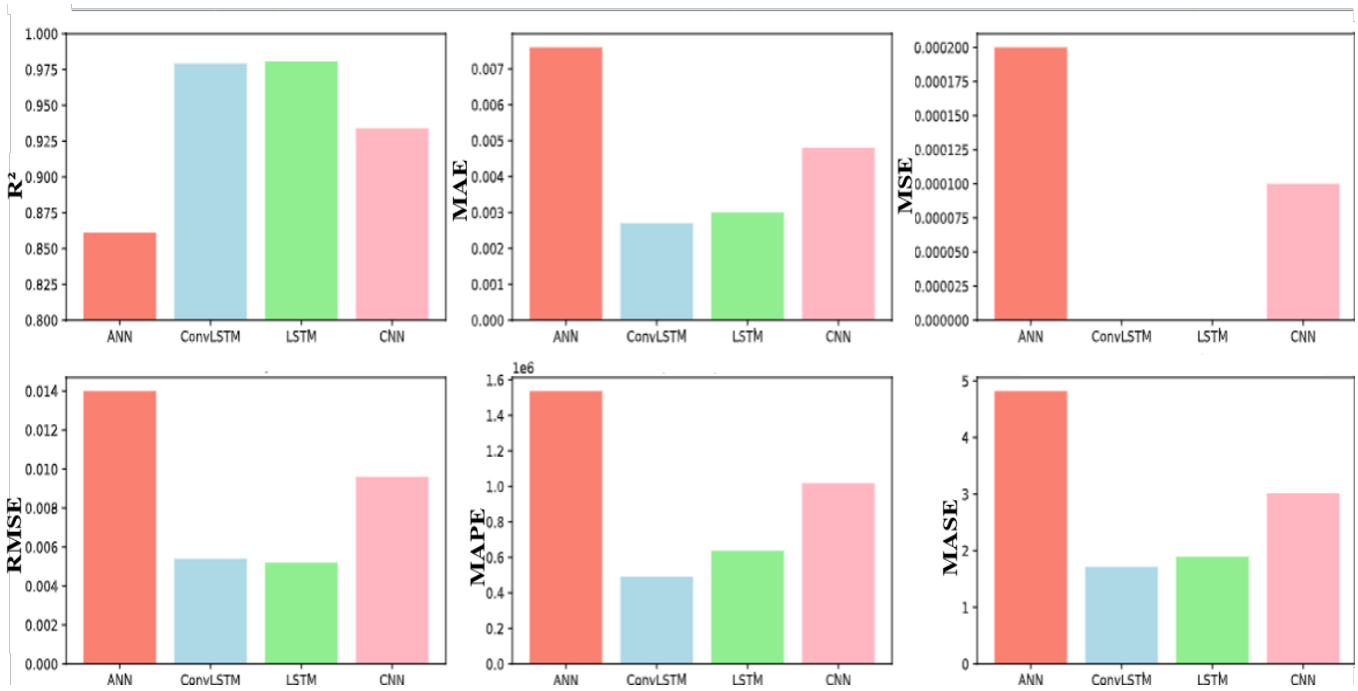

Figure 8: Comparing the performance of the models

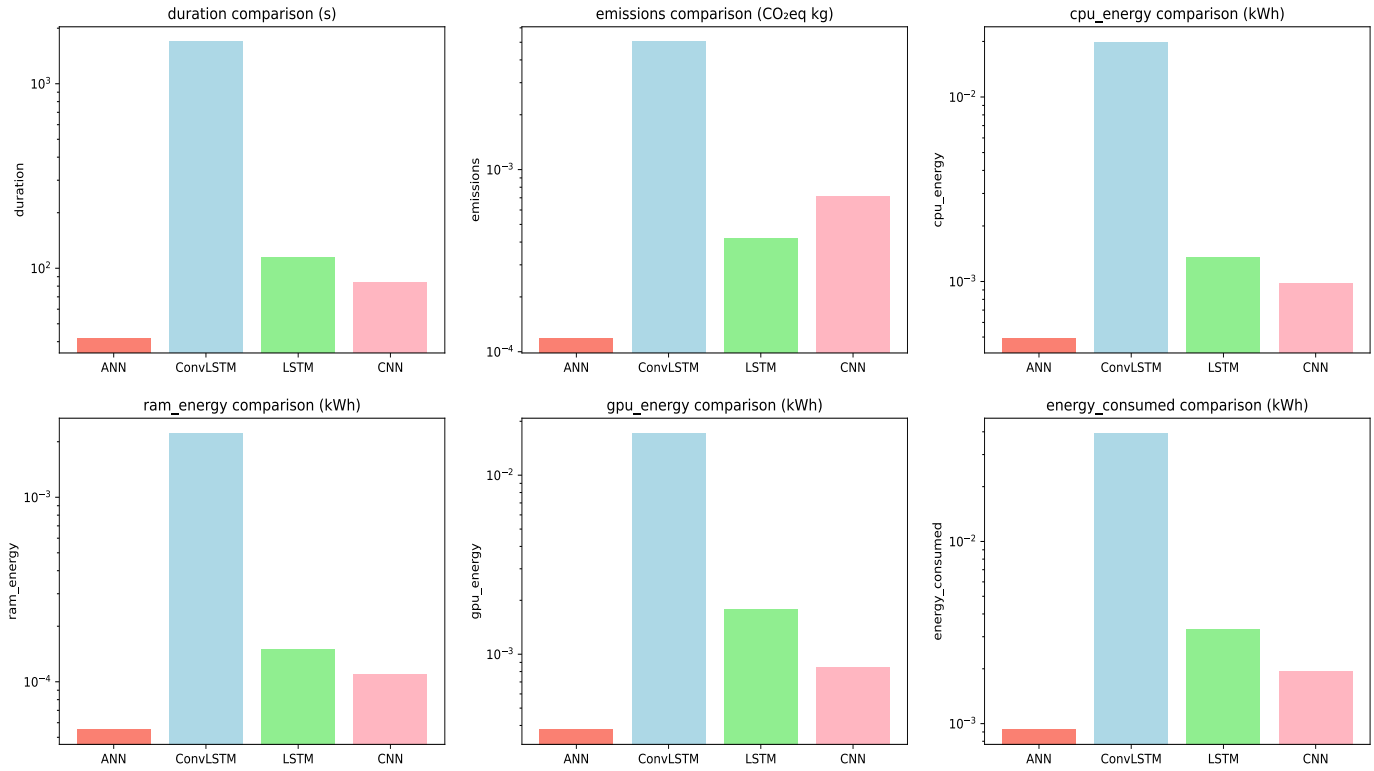

Figure 9: Comparative results of energy consumption and CO_2 emissions during model training

AI for renewable energy systems: balancing predictive accuracy with environmental responsibility. As shown in Fig 10, the standalone LSTM model achieves near-optimal accuracy (R^2 = 0.971) while maintaining minimal computational costs (0.85 kWh energy, 45 gCO_2eq emissions). In contrast, the hybrid CNN-LSTM model provides only a marginal improvement in R^2 (0.975), a gain of just 0.4%, at a disproportionately high environmental cost. It consumes 32% more energy (1.45 kWh) and produces 69% higher CO_2 emissions (76 gCO_2eq). This significant divergence illustrates a diminishing returns effect, where the hybrid model's architectural complexity (60,000 parameters vs. LSTM's 129,000) introduces considerable overhead without a proportional accuracy gain. The LSTM model ranks highest in the TOPSIS evaluation due to its superior balance of accuracy, energy efficiency, and low carbon footprint, making it a pragmatic choice for most winter house applications. However, the hybrid model's slight accuracy advantage may be critical in specific scenarios requiring spatial-temporal granularity, such as predicting PV output during rapid snowmelt events or multi-facade shading dynamics. For example, in cases where localized snow accumulation on south-facing panels creates micro-variations in production, the CNN's spatial feature extraction could enhance short-term forecasting.

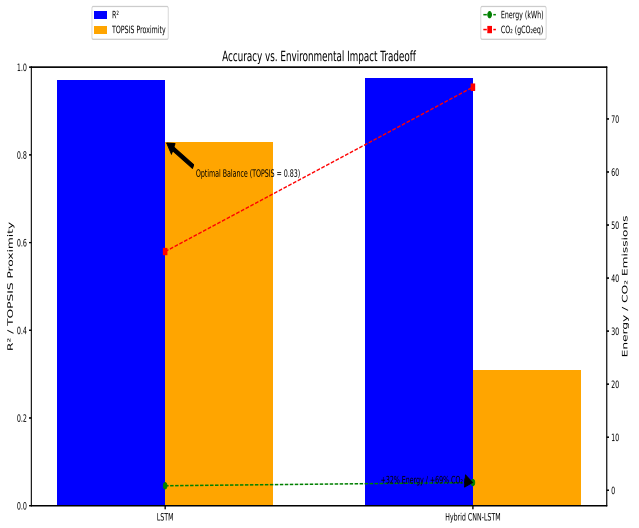

Figure 10: Tradeoff between predictive accuracy and environmental impact for LSTM and hybrid CNN-LSTM models.

Table 5: Criteria and their assigned weights.

Criteria	Weight
duration	0.05
emissions	0.2
energy consumed	0.2
model size	0.2
MAE	0.05
MSE	0.05
RMSE	0.05
MAPE	0.05
MASE	0.05
R^2	0.1

Recent research underscores the importance of tracking the environmental impact of software development. For example, Sevilla Martinez et al. (36) investigated the CO_2 emissions of training convolutional neural networks for autonomous driving, highlighting the need for energy-efficient algorithms and emphasizing energy efficiency as a measure of model quality. They utilized CodeCarbon to measure carbon emissions associated with their training process, demonstrating the tool's utility in quantifying the environmental footprint of machine learning models. Similarly, Sousa et al. (37) employed CodeCarbon to evaluate CO_2 emission rates for their deep learning models (ConformalLayers). They found that ConformalLayers-based networks had lower emission rates than their conventional counterparts, especially as network depth increased, thus showcasing the potential of architectural choices to impact the environmental sustainability of software systems.

4.3. Performance of PV Prediction models and comparison with conventional software tools

This section evaluates the performance of our selected low-carbon prediction model, a lightweight LSTM, in predicting PV production for the Swiss winter house (Fig. 1) during the winter period. The proposed model is compared to established software such as BIMsolar and PVSyst (13). Fig. 11 provides a monthly comparison of actual PV production against the predictions of our model and the benchmark software. The LSTM model effectively captures seasonal production trends, especially during the winter, while BIMsolar and PVSyst systematically underestimate production during this critical period, as noted by Othman et al. (38). The LSTM model's predictions align more closely with actual production, demonstrating its superior performance over traditional software. This variability of solar energy production in snowy regions highlights the influence of seasonal weather conditions on PV systems, emphasizing the need for empirical models, as advocated by Nazzareno Diodato et al. (39), especially in climates such as the central Mediterranean. The importance of optimized prediction models for accurate PV integration, especially in winter house projects, is further reinforced by the quantitative evaluation presented in Table 6. This table compares the mod-

els using standard metrics (MSE, R^2, MAE, MAPE), demonstrating that LSTM achieves higher accuracy, with predictions closer to real values than those of BIMSOLAR and PVSYST. The lower computational requirements of LSTM compared to other deep learning models like CNNs and ConvLSTMs align with our low-carbon goal, extending from the prediction model itself to building decarbonization through efficient PV integration. Furthermore, we analyze the relative deviations between actual production and predictions of our LSTM model, BIMSOLAR, and PVSyst (Fig. 12). These deviations highlight the challenges faced by conventional software, especially in winter when weather conditions are highly variable. As highlighted by Salimi et al. (16) and Li et al. (17), dynamic and localized data are essential for accurate prediction, outperforming generic Typical Meteorological Year (TMY) data-based approaches commonly used in conventional software. These results highlight the need for optimized prediction models like our lightweight LSTM, especially for PEWH winter houses, to enable efficient and sustainable integration of renewable energy. While our hybrid CNN-LSTM model demonstrates strong performance for PV energy prediction in winter conditions, preliminary investigations indicate that its generalization to drastically different climates (e.g., arid or tropical regions) and architectural configurations (e.g., high-density urban buildings) remains unvalidated. Consequently, future work will explore the integration of advanced architectures such as Time Convolutional Networks (TCNs) and Transformers. These models have shown promise in capturing long-term temporal dependencies and could further improve prediction accuracy in highly variable environments. Preliminary investigations into TCNs are already underway, and a comparative analysis of their computational efficiency, carbon footprint, and robustness in snowy climates will be included in subsequent studies. In addition, alignment with ISO 14064 carbon accounting standards will be pursued to strengthen the benchmarking against global sustainability metrics, filling a critical gap in AI-driven renewable energy systems. These extensions, together with a comparative analysis of computational efficiency and carbon footprint, will provide a more comprehensive assessment of state-of-the-art approaches for PV power predicting.

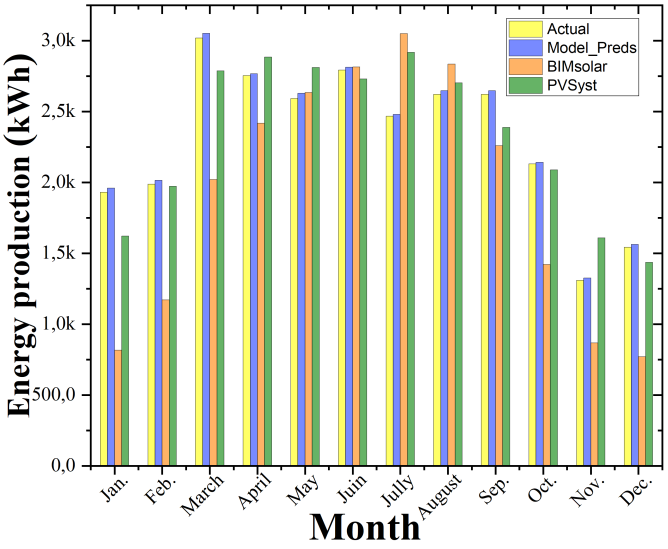

Figure 11: Monthly PV Output Comparison: monthly PV production on a south-facing roof by various AI model and sizing software tools.

Table 6: Comparison of performance metrics of PV prediction models.

Model	MSE	R2	MAE	MAPE
LSTM	570.41	0.997	22.416	0.0099
BIMSOLAR	403237.08	-0.5621	534.75	0.257
PVSYST	48796.83	0.8109	181.83	0.085

4.4. Analysis of Energy Efficiency and Decarbonization Potential

To optimize PV installation strategies for positive energy winter homes (PEWH), The energy efficiency and decarbonization potential of various configurations using data from a PEWH case study. This house is currently equipped with PV panels on all facades (south, east, west, and north) and roof sections (south and north), providing real-world data on PV production, energy consumption, and grid feed-in for each building component. This comprehensive dataset, combined with our predictive model, allows us to develop optimized decarbonization scenarios, avoiding energy overproduction and accounting for embodied carbon emissions associated with PV manufacturing and transportation. Table 7 compares primary energy consumption and GHG emissions with and without PV panels. Without PV panels, the house is entirely dependent on the Swiss electricity mix, resulting in a primary energy consumption of 727.03 $kWhep/m^2SU.year$. The integration of PV panels significantly reduces this consumption to 266.25 $kWhep/m^2SU.year$ (a reduction of 63%), even without battery storage. While 36% of the house's energy needs are still met by the grid, this substantial reduction demonstrates the effectiveness of PV systems in meeting the energy demands of buildings, consistent with the reported energy savings of 20 to 50% through the integration of renewables (1; 40). The environmental impact is equally significant. Without PV, GHG

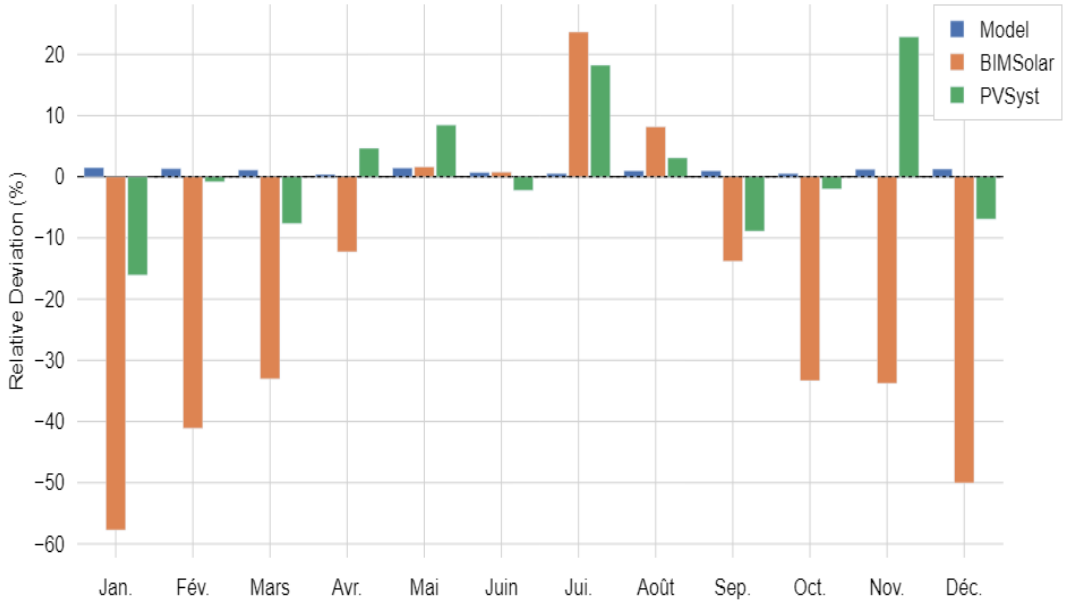

Figure 12: Comparison of the Effectiveness of PVSyst, BIMSOLAR and the Lightweight LSTM Model in Estimating the Monthly PV Energy Production of a PEWH House: Relative Deviation Between Actual and Estimated Monthly PV Energy Production

Table 7: Decarbonization Potential of PV Panels: Primary Energy and GHG Emission Reduction in a PEWH House

	Electricity consumption in primary energy ($kWhep/mS\,U.year$)	**GHG emissions from Consumption electricity** ($kgeqCO_2/m^2S\,U.year$)	**Decarbonization rate (%)**
Without PV Panels	727.03	16.44	0

	Electricity consumption in primary energy (Grid cover) ($kWhep/mS\,U.year$)	**GHG emissions from Electricity covered by Grid energy** ($kgeqCO_2/m^2S\,U.year$)	**GHG emissions from Electricity Directly consumed** ($kgeqCO_2/m^2S\,U.year$)	**Decarbonization rate (%)**
With PV Panels	266.25	6.02	8.61	11

emissions reach 16.44 $kgeqCO_2/m^2S\,U.year$. With PV integration, GHG grid-supplied electricity emissions decrease to 6.02 $kgeqCO_2/m^2.S\,U.year$. The electricity consumption of the PV system, including embodied carbon, contributes 8.61 $kgeqCO_2/m^2.S\,U.year$. This translates to a net decarbonization rate of 11%, as shown in Table 7. Although this is a significant improvement, this lower rate compared to studies excluding embodied carbon (41; 42) highlights the importance of considering the full lifecycle emissions of the panel before its integration into the winter house PEWH. Nevertheless, the transition from 0% to 11% decarbonization demonstrates the positive impact of PV integration. This reduction in grid supplied and PV related emissions highlights environmental benefits, consistent with trends observed in studies of renewable energy systems (43).

In regions with heavy snowfall, our study shows that installing panels on all façades can lead to overproduction and an undesirable increase in the carbon footprint. On the other hand, by opting for targeted configurations such as installing them exclusively on the south façade or on the north roof, it is possible to adjust the production to the actual needs of the building. These optimized configurations improve the decarbonization rate (with observed rates of 131% and 116%, respectively) while reducing energy waste, thus providing an optimal balance between production and environmental impact. Recent studies have advanced the use of deep learning for PV predicting; for example, Kumar et al. (44) demonstrate the application of AI to improve PV system performance, and other researchers have proposed hybrid models to improve forecast accuracy (45). However, these works generally neglect the environmental costs associated with model training and operation. In contrast, our study fills this gap by integrating a carbon footprint assessment via the CodeCarbon library and applying the TOPSIS framework for multi-criteria model selection. This integrated approach not only improves forecast accuracy but also ensures that the selected model minimizes energy consumption

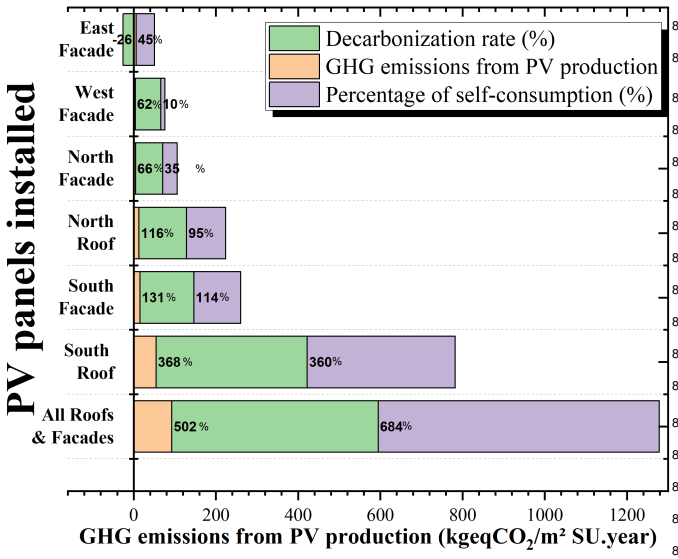

Figure 13: Decarbonization of PEWH houses with different installation configurations of PV panels on the facade or on the roof

and CO_2 emissions, achieving a reduction in primary energy consumption of up to 63% and decarbonization rates of up to 131%. Such a dual focus on technical performance and environmental sustainability represents a significant advance in sustainable AI for renewable energy applications. Further analysis will explore optimized PV configurations to maximize decarbonization while minimizing overproduction and its associated environmental impact. Fig. 13 highlights the significant potential of PV installations to reduce greenhouse gas (GHG) emissions and improve decarbonization in Swiss winter homes (PEWH). Optimizing PV production using lightweight deep learning models further amplifies the environmental benefits of this technology. We analyze two scenarios: the current configuration and an optimized configuration.

Current Scenario: Overproduction and Counterproductive Decarbonization:

The current scenario (Fig. 13) depicts the house with PV panels installed on all facades and roof sections. While this maximizes self-consumption, except during winter nights, it also results in substantial overproduction, exceeding the annual primary energy consumption of 727 $kWhep/m^2SU.year$ by over 600%, reaching an excess of 93 $kgeqCO_2/m^2.SU.year$ in GHG emissions (Fig. 13). This overproduction, coupled with the embodied carbon of the extensive PV system, leads to a decarbonization penalty of 502%. This counterproductive outcome highlights the critical importance of considering the entire lifecycle emissions of PV panels, including manufacturing and transport. When overproduction is this significant, it negates the environmental benefits of on-site generation, demonstrating that simply maximizing PV coverage can be detrimental to overall decarbonization efforts. A more nuanced approach is required to balance energy production with actual needs and minimize the environmental impact of embodied carbon.

Optimized Scenario: Balancing Production and Decarbonization:

To address the shortcomings of the current scenario, alternative PV configurations were explored using the lightweight LSTM deep learning model (Section 4.2 and Section 4.3), selected for its energy efficiency and low carbon footprint. The results, presented in Fig. 13, suggest two primary optimized configurations: PV installations solely on the south facade or solely on the north roof. These configurations achieve decarbonization rates of 131% and 116%, respectively, while covering 114% and 95% of the energy consumption needs, respectively.

These slightly higher-than-required production levels remain reasonable, ensuring sufficient energy supply while minimizing overproduction. The south facade configuration yields GHG emissions of 15 $kgeqCO_2/m^2.SU.year$, while the north roof configuration results in 4.12 $kgeqCO_2/m^2.SU.year$.

A less conventional scenario, considering the typical south-facing preference for PV installations, involves a combined installation on the east, west, and north facades, covering 45%, 10%, and 35% of energy needs, respectively, for a total coverage of 90%. This configuration results in respective GHG emissions of 6, 4, and 4 $kgeqCO_2/m^2.SU.year$, totaling 14 $kgeqCO_2/m^2.SU.year$. Although this scenario seems promising on an annual basis, it cannot meet instantaneous or daily energy demands with this distributed configuration and could prove difficult in practice. Therefore, the south or north facade/roof configurations remain the most credible optimized scenarios.

The optimized scenarios offer several key advantages:

- Reduced GHG Emissions: Minimizing unnecessary PV installations reduces the overall environmental impact associated with embodied carbon.
- Improved Energy Utilization: Balancing PV production with actual consumption avoids overproduction and maximizes the efficient use of generated electricity.
- Enhanced Decarbonization Efficiency: The positive decarbonization rates achieved by the south and north facade/roof configurations (exceeding 100%) demonstrate the potential for significant carbon footprint reduction through optimized PV integration. These scenarios achieve high decarbonization and self-sufficiency while accounting for full lifecycle emissions of the installed panels.

These findings have important implications for sustainable building design, especially in regions like Switzerland with unique challenges for PV production. Carefully selecting PV installation locations and optimizing production using environmentally conscious deep learning models maximizes the benefits of PV technology and contributes to a more sustainable energy future.

5. Conclusion

This study presented a innovative approach for optimizing PV energy production in winter houses using lightweight deep learning models while prioritizing environmental sustainability. By integrating carbon footprint assessments with predictive accuracy, we demonstrated a 63% reduction in primary energy consumption and achieved decarbonization rates of up to 131% through strategic PV panel placement on south facades or north roofs. Our hybrid CNN-LSTM model proved highly effective in winter conditions, outperforming traditional software like PVsyst and BIMSolar, which systematically underestimated production in snowy environments. These results underscore the potential of AI-driven models to balance energy efficiency with low-carbon practices, addressing both overproduction challenges and embodied emissions from PV systems. Looking ahead, further investigations could integrate advanced battery management and real-time satellite weather feeds to refine predictive reliability and grid autonomy. Expanding this methodology to diverse climates such as arid or coastal regions and architectural designs (e.g., industrial buildings) would solidify its global relevance for solar optimization. Bridging AI innovation with sustainable engineering, this work lays the groundwork for intelligent, climate-resilient energy systems, driving progress toward carbon-neutral infrastructure even in extreme environments.

Acknowledgements

The authors sincerely thank CESI Région Est and the CESI LINEACT laboratory, France, for their invaluable support of this research. Special gratitude is extended to Nadia Vontobel for her generous provision of the data utilized in this study.

References

[1] A. Savvides, C. Vassiliades, A. Michael, S. Kalogirou, Siting and building-massing considerations for the urban integration of active solar energy systems, Renewable Energy 135 (2019) 963–974. doi:https://doi.org/10.1016/j.renene.2018.12.017.

[2] R. Zhu, C. Cheng, P. Santi, M. Chen, X. Zhang, M. Mazzarello, M. S. Wong, C. Ratti, Optimization of photovoltaic provision in a three-dimensional city using real-time electricity demand, Applied Energy 316 (2022) 119042. doi:https://doi.org/10.1016/j.apenergy.2022.119042.

[3] R. E. Ashmawy, N. Y. Azmy, Buildings orientation and its impact on the energy consumption, ARCHive-SR 2 (3) (2018) 35–49.

[4] C. Vassiliades, A. Michael, A. Savvides, S. Kalogirou, Improvement of passive behaviour of existing buildings through the integration of active solar energy systems, Energy 163 (2018) 1178–1192. doi:https://doi.org/10.1016/j.energy.2018.08.148.

[5] R. E. Pawluk, Y. Chen, Y. She, Photovoltaic electricity generation loss due to snow – a literature review on influence factors, estimation, and mitigation, Renewable and Sustainable Energy Reviews 107 (2019) 171–182. doi:https://doi.org/10.1016/j.rser.2018.12.031.

[6] A. Rahmatmand, S. J. Harrison, P. H. Oosthuizen, Numerical and experimental study of an improved method for prediction of snow melting and snow sliding from photovoltaic panels, Applied Thermal Engineering 158 (2019) 113773. doi:https://doi.org/10.1016/j.applthermaleng.2019.113773.

[7] K. S. Hayibo, A. Petsiuk, P. Mayville, L. Brown, J. M. Pearce, Monofacial vs bifacial solar photovoltaic systems in snowy environments, Renewable Energy 193 (2022) 657–668. doi:https://doi.org/10.1016/j.renene.2022.05.050.

[8] L. Stefan, he effect of weather on solar technology adoption, Environmental and Resource Economics 84 (2023) 1179–1219. doi:10.1007/s10640-022-00753-3.

[9] L. Walker, J. Hofer, A. Schlueter, High-resolution, parametric bipv and electrical systems modeling and design, Applied Energy 238 (2019) 164–179. doi:https://doi.org/10.1016/j.apenergy.2018.12.088.

[10] M. Dourhmi, B. Kaoutar, A. Ilyass, Z. Mourad, M. Tawfik, J. Youssef, Improved hourly prediction of bipv photovoltaic power building using artificial learning machine: A case study, Ben Ahmed, M., Abdelhakim, B.A., Ane, B.K., Rosiyadi, D. (eds) Emerging Trends in Intelligent Systems and Network Security 147 (2023). doi:10.1007/978-3-031-15191-$0_2$6.

[11] A novel approach to reduce both front and rear side power losses in perc solar cells using different combinations of transparent metal oxides, Ceramics International 49 (2) (2023) 2821–2828. doi:https://doi.org/10.1016/j.ceramint.2022.09.264.

[12] J. Polo, M.-C. Nuria, A.-A. Miguel, S.-S. Carlos, C. José, de la Cruz Marina, Exploring the pv power forecasting at building façades using gradient boosting methods, Energies 16 (3) (2023). doi:10.3390/en16031495.

[13] A. Ilyass, J. Youssef, Photogrammetry and deep learning for energy production prediction and building-integrated photovoltaics decarbonization, Building Simulation 17 (2024). doi:10.1007/s12273-023-1089-y.

[14] D. Kumar Dhaked, V. Narayanan, R. Gopal, O. Sharma, S. Bhattarai, S. Dwivedy, Exploring deep learning methods for solar photovoltaic power output forecasting: A review, Renewable Energy Focus 53 (2025) 100682. doi:https://doi.org/10.1016/j.ref.2025.100682.

[15] D. González-Peña, I. García-Ruiz, M. Díez-Mediavilla, M. I. Dieste-Velasco, C. Alonso-Tristán, Photovoltaic prediction software: Evaluation with real data from northern spain, Applied Sciences 11 (11) (2021). doi:10.3390/app11115025.

[16] A. Mosavi, M. Salimi, S. Faizollahzadeh Ardabili, T. Rabczuk, S. Shamshirband, A. R. Varkonyi-Koczy, State of the art of machine learning models in energy systems, a systematic review, Energies 12 (7) (2019). doi:10.3390/en12071301.

[17] F. Li, H. Zheng, X. Li, A novel hybrid model for multi-step ahead photovoltaic power prediction based on conditional time series generative adversarial networks, Renewable Energy 199 (2022) 560–586. doi:https://doi.org/10.1016/j.renene.2022.08.134.

[18] A. H. Al-Waeli, H. A. Kazem, J. H. Yousif, M. T. Chaichan, K. Sopian, Mathematical and neural network models for predicting the electrical performance of a pv/t system, International Journal of Energy Research 43 (14) (2019) 8100–8117. doi:https://doi.org/10.1002/er.4807.

[19] S. Jeon, H. Kang, S. Song, S. Kim, Method to establish time-series building energy data inventory based on frequency for energy-sharing community planning, Solar Energy 276 (2024) 112693. doi:https://doi.org/10.1016/j.solener.2024.112693.

[20] M. Tawalbeh, A. Al-Othman, F. Kafiah, E. Abdelsalam, F. Almomani, M. Alkasrawi, Environmental impacts of solar photovoltaic systems: A critical review of recent progress and future outlook, Science of The Total Environment 759 (2021) 143528. doi:https://doi.org/10.1016/j.scitotenv.2020.143528.

[21] B. Liu, X. Huo, Prediction of photovoltaic power generation and analyzing of carbon emission reduction capacity in china, Renewable Energy 222 (2024) 119967. doi:https://doi.org/10.1016/j.renene.2024.119967.

[22] C. You, S. I. Khattak, M. Ahmad, Impact of innovation in solar photovoltaic energy generation, distribution, or transmission-related technologies on carbon dioxide emissions in china, Journal of the Knowledge Economy 15 (1) (2024) 3600–3634. doi:10.1007/s13132-023-01284-y.

[23] Yin2024, Green ai: exploring carbon footprints, mitigation strategies, and trade offs in large language model training, Discover Artificial Intelligence 4 (1) (2024) 49. doi:10.1007/s44163-024-00149-w.

[24] A. S. Luccioni, A. Hernandez-Garcia, Counting carbon: A survey of factors influencing the emissions of machine learning, ArXiv abs/2302.08476 (2023). URL `https://api.semanticscholar.org/CorpusID:256900966`

[25] A. Martiny, Towards sustainable ai: Monitoring and analysis of carbon emissions in machine learning algorithms, Master's degree thesis, Politecnico di Torino, Turin, Italy, master's Degree in ICT for Smart Societies (July 2023).

[26] Z. Li, F. Liu, W. Yang, S. Peng, J. Zhou, A survey of convolutional neural networks: analysis, applications, and prospects, IEEE transactions on neural networks and learning systems 33 (12) (2021) 6999–7019.

[27] I. Abouelaziz, A. Chetouani, M. El Hassouni, L. J. Latecki, H. Cherifi, No-reference mesh visual quality assessment via ensemble of convolutional neural networks and compact multi-linear pooling, Pattern Recognition 100 (2020)

107174.
[28] Y. Sun, V. Venugopal, A. R. Brandt, Short-term solar power forecast with deep learning: Exploring optimal input and output configuration, Solar Energy 188 (2019) 730–741. doi:https://doi.org/10.1016/j.solener.2019.06.041.
[29] Y. Yu, X. Si, C. Hu, J. Zhang, A review of recurrent neural networks: Lstm cells and network architectures, Neural computation 31 (7) (2019) 1235–1270.
[30] S. Hochreiter, Long short-term memory, Neural Computation MIT-Press (1997).
[31] F. Asdrubali, G. Baldinelli, F. D'Alessandro, F. Scrucca, Life cycle assessment of electricity production from renewable energies: Review and results harmonization, Renewable and Sustainable Energy Reviews 42 (2015) 1113–1122. doi:https://doi.org/10.1016/j.rser.2014.10.082.
[32] N. Scarlat, M. Prussi, M. Padella, Quantification of the carbon intensity of electricity produced and used in europe, Applied Energy 305 (2022) 117901. doi:https://doi.org/10.1016/j.apenergy.2021.117901.
[33] S. Savazzi, V. Rampa, S. Kianoush, M. Bennis, An energy and carbon footprint analysis of distributed and federated learning, IEEE Transactions on Green Communications and Networking 7 (1) (2023) 248–264. doi:10.1109/TGCN.2022.3186439.
[34] N. I. Ilham, N. Y. Dahlan, M. Z. Hussin, Optimizing solar pv investments: A comprehensive decision-making index using critic and topsis, Renewable Energy Focus 49 (2024) 100551. doi:https://doi.org/10.1016/j.ref.2024.100551.
[35] H. Kaur, S. Gupta, A. Dhingra, Selection of solar panel using entropy topsis technique, Materials Today: Proceedings (2023). doi:https://doi.org/10.1016/j.matpr.2023.02.034.
[36] F. S. Martínez, R. Parada, J. Casas-Roma, Co2 impact on convolutional network model training for autonomous driving through behavioral cloning, Advanced Engineering Informatics 56 (2023) 101968. doi:https://doi.org/10.1016/j.aei.2023.101968.
[37] E. V. Sousa, C. N. Vasconcelos, L. A. Fernandes, An analysis of conformal-layers' robustness to corruptions in natural images, Pattern Recognition Letters 166 (2023) 190–197. doi:https://doi.org/10.1016/j.patrec.2022.11.002.
[38] R. Othman, T. M. Hatem, Assessment of pv technologies outdoor performance and commercial software estimation in hot and dry climates, Journal of Cleaner Production 340 (2022) 130819. doi:https://doi.org/10.1016/j.jclepro.2022.130819.
[39] N. Diodato, F. C. Ljungqvist, G. Bellocchi, Empirical modelling of snow cover duration patterns in complex terrains of italy, Theoretical and Applied Climatology 147 (2022) 1195–1212. doi:https://doi.org/10.1007/s00704-021-03867-8.
[40] Y. Li, V. Arulnathan, M. Heidari, N. Pelletier, Design considerations for net zero energy buildings for intensive, confined poultry production: A review of current insights, knowledge gaps, and future directions, Renewable and Sustainable Energy Reviews 154 (2022) 111874. doi:https://doi.org/10.1016/j.rser.2021.111874.
[41] L. Dong, Y. Gu, K. Cai, X. He, Q. Song, W. Yuan, H. Duan, Unveiling lifecycle carbon emissions and its mitigation potentials of distributed photovoltaic power through two typical case systems, Solar Energy 269 (2024) 112360. doi:https://doi.org/10.1016/j.solener.2024.112360.
[42] L. Yuan, P. Nain, M. Kothari, A. Anctil, Material intensity and carbon footprint of crystalline silicon module assembly over time, Solar Energy 269 (2024) 112336. doi:https://doi.org/10.1016/j.solener.2024.112336.
[43] M. Tawalbeh, A. Al-Othman, F. Kafiah, E. Abdelsalam, F. Almomani, M. Alkasrawi, Environmental impacts of solar photovoltaic systems: A critical review of recent progress and future outlook, Science of The Total Environment 759 (2021) 143528. doi:https://doi.org/10.1016/j.scitotenv.2020.143528.
[44] A. Kumar, A. K. Dubey, I. Segovia Ramírez, et al., Artificial intelligence techniques for the photovoltaic system: A systematic review and analysis for evaluation and benchmarking, Archives of Computational Methods in Engineering 31 (2024) 4429–4453. doi:10.1007/s11831-024-10125-3.
[45] D. Salman, C. Direkoglu, M. Kusaf, et al., Hybrid deep learning models for time series forecasting of solar power, Neural Computing and Applications 36 (2024) 9095–9112. doi:10.1007/s00521-024-09558-5.